Proc. Nat. Acad. Sci. USA
Vol. 72, No. 4, pp. 1291–1295, April 1975

Stochastics of Cycle Completions (Fluxes) in Biochemical Kinetic Diagrams

(membrane transport/chemical reactions/steady-state kinetics/Monte Carlo simulation/fluctuations/noise)

TERRELL L. HILL AND YI-DER CHEN

Laboratory of Molecular Biology, National Institute of Arthritis, Metabolism, and Digestive Diseases, National Institutes of Health, Bethesda, Maryland 20014

Contributed by Terrell L. Hill, January 21, 1975

ABSTRACT **Over a long time period, the rate constants for cycle completions (one-way fluxes) in steady-state biochemical diagrams can be expressed explicitly in terms of the elementary rate constants for transitions between states of the diagram. These cycle rate constants determine the mean one-way fluxes in the diagram and also fluctuations about the means. These properties are confirmed by Monte Carlo computer simulations on special cases. Two other topics are considered briefly: the effect of the starting state or states on the numbers of cycle completions in computer simulation runs; and the more detailed stochastic approach required if individual cycle completions are to be followed (i.e., if the "long time" restriction is removed).**

In several biochemical problems, for example, muscle contraction (1) and active transport (2), a certain "central" macromolecule or macromolecular complex can exist in a finite number of discrete states, with possible inverse pairs of transitions between some pairs of states. It is convenient (3) to define first-order rate constants for all of these transitions. We use the rate-constant notation α_{ij} for the transition from state i to state j. The states and rate constants form a "diagram", illustrated in Fig. 1, which in general contains one or more cycles. The diagram in Fig. 1 has six cycles, for example. In cases of biological interest, there is an ensemble of these macromolecular systems and the rate constants α_{ij} for each system have values that lead to a steady state, rather than to equilibrium, after a transient period, with non-zero net mean flux around some or all of the cycles. These fluxes correspond to net membrane transport, net chemical reaction, etc.

In an earlier paper (3), relations between free energies of macromolecular states and the rate constants α_{ij} were emphasized. Also included was an introduction to a stochastic treatment of steady-state cycle kinetics. The present paper is a continuation of this stochastic treatment.

The point of view here is essentially "experimental". That is, we report on Monte Carlo computational properties for a few special cases. Our object is, first, to verify the simple theory presented in the previous paper (3) and then to present two new kinds of computational results for systems of this type.

Review of stochastic treatment of cycles

We summarize here the notation and basic ideas already introduced (3). Imagine that we follow in detail a single system over a long period of time, as it occasionally and instantaneously changes from one state to another of its kinetic diagram, in accordance with the first-order transition probabilities α_{ij} of the diagram. The diagram has cycles labeled $\alpha, \beta, \gamma, \ldots$. From time to time, one or another of the cycles is completed. Over a very long period of time, let $p_{\alpha+}, p_{\alpha-}, p_{\beta+}, p_{\beta-}, \cdots$ be the fraction of completed cycles of type α in direction + (assigned by some convention), etc. The sum of these probabilities is unity. Also, let τ be the mean time between cycles. Then the probability of completing any cycle in the infinitesimal interval dt is dt/τ, while the probability of completing a cycle of type $\alpha+$, $\alpha-$, etc., in dt is $p_{\alpha+}dt/\tau$, $p_{\alpha-}dt/\tau$, etc. Thus, if we denote the first-order rate constants for *cycle completions* by $k_{\alpha+}$, $k_{\alpha-}$, etc., we have $k_{\alpha+} = p_{\alpha+}/\tau$, $k_{\alpha-} = p_{\alpha-}/\tau$, etc.

In an ensemble of N equivalent and independent systems (e.g., a membrane sample with N macromolecular carriers), the mean numbers of cycles of each type completed per unit time are $J_{\alpha+} = Nk_{\alpha+}, J_{\alpha-} = Nk_{\alpha-}$, etc. The *net* cycle fluxes are then

$$J_\alpha = N(k_{\alpha+} - k_{\alpha-}), \text{ etc.} \qquad [1]$$

The stochastic cycle properties introduced above may be expressed in terms of the single-transition rate constants α_{ij} of the diagram. Using the diagram method (2), the *net* fluxes can always be written in the form

$$\begin{aligned} J_\alpha &= N(\Pi_{\alpha+} - \Pi_{\alpha-})\Sigma_\alpha/\Sigma \\ J_\beta &= N(\Pi_{\beta+} - \Pi_{\beta-})\Sigma_\beta/\Sigma, \end{aligned} \qquad [2]$$

etc., where Σ is the sum of directional diagrams (2) for all states, $\Pi_{\alpha+}$ is the product of rate constants around cycle α in the + direction, $\Pi_{\alpha-}$ is the product of rate constants around cycle α in the − direction, $(\Pi_{\alpha+} - \Pi_{\alpha-})\Sigma_\alpha$ is the sum of cycle flux diagrams (this defines Σ_α), etc. The expressions for $\Pi_{\alpha+}, \Pi_{\alpha-}, \Sigma_\alpha, \Sigma$, etc., involve the α_{ij} only (2).

Eq. **2a** gives the mean *net* flux around cycle α. Actually, we can go further and identify $N\Pi_{\alpha+}\Sigma_\alpha/\Sigma$ with the mean flux around cycle α in the + direction ($J_{\alpha+}$) by noting that $J_\alpha \to N\Pi_{\alpha+}\Sigma_\alpha/\Sigma$ if we let any one of the rate constants in Π_- become very small. This is a crucial identification which is not obvious *a priori*. The argument just mentioned is slightly suspect because the particular rate constant in Π_- that is used is also included in Σ (as are *all* the α_{ij}). We shall return to this point below.

Using this result for the one-way fluxes, the cycle rate constants are given explicitly in terms of the α_{ij} by

$$\begin{aligned} k_{\alpha+} &= \Pi_{\alpha+}\Sigma_\alpha/\Sigma = J_{\alpha+}/N, \\ k_{\alpha-} &= \Pi_{\alpha-}\Sigma_\alpha/\Sigma = J_{\alpha-}/N, \end{aligned} \qquad [3]$$

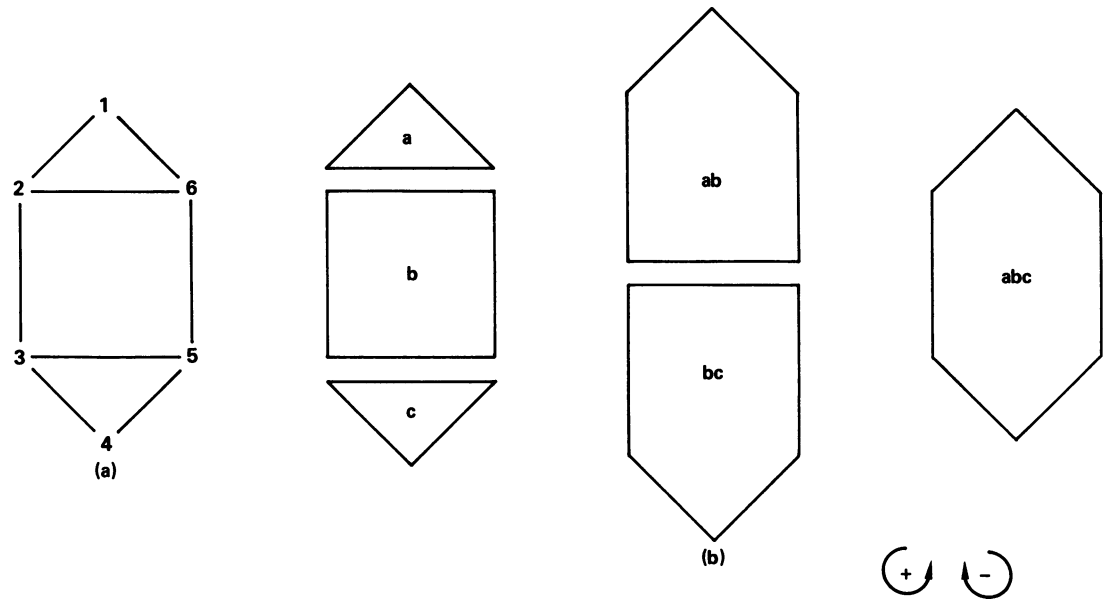

FIG. 1. (a) Illustrative kinetic diagram with six states. Each line represents forward and backward transitions. (b) The six cycles belonging to the diagram in (a). The + and − flux directions (for all cycles) are arbitrarily assigned as shown.

etc. The cycle probabilities introduced above become, then,

$$p_{\alpha+} = \tau k_{\alpha+} = \tau \Pi_{\alpha+} \Sigma_\alpha / \Sigma, \qquad p_{\alpha-} = \tau \Pi_{\alpha-} \Sigma_\alpha / \Sigma, \quad [4]$$

etc. Since the sum of these probabilities is unity,

$$\begin{aligned} \tau &= (k_{\alpha+} + k_{\alpha-} + k_{\beta+} + \cdots)^{-1} \\ &= \Sigma / (\Pi_{\alpha+} \Sigma_\alpha + \Pi_{\alpha-} \Sigma_\alpha + \Pi_{\beta+} \Sigma_\beta + \cdots). \end{aligned} \quad [5]$$

Over a long enough time interval, cycle completions of each type, α_+, α_-, β_+, etc., may be regarded as independent random events, each with a Gaussian frequency distribution (3). Thus, if $P(r_{\alpha+},t)$ is the probability of observing $r_{\alpha+}$ cycles of type $\alpha+$ after a long time t, $P(r_{\alpha+},t)$ is a Gaussian function in $r_{\alpha+}$ with mean and variance (3).

$$\bar{r}_{\alpha+} = \sigma_{\alpha+}^2 = k_{\alpha+} t = J_{\alpha+} t/N, \text{ etc.} \quad [6]$$

Similarly, for combinations such as the *net* number of α cycles, we have the Gaussian distribution parameters

$$\begin{aligned} \bar{r}_\alpha &= \bar{r}_{\alpha+} - \bar{r}_{\alpha-} = (k_{\alpha+} - k_{\alpha-}) t = J_\alpha t/N \\ \sigma_\alpha^2 &= \bar{r}_{\alpha+} + \bar{r}_{\alpha-} = (k_{\alpha+} + k_{\alpha-}) t. \end{aligned} \quad [7]$$

A final topic. Let p_i be the steady-state probability that a given system is in state i. The p_i are determined by the α_{ij} via the diagram method (2, 3, 4). Let f_i be the fraction of all transitions that start from state i. Also, let τ_{tr} be the mean time between all transitions, and let $\tau_{tr}^{(i)}$ be the mean time between transitions when the starting state is i. The latter quantity is just the reciprocal of the sum of the *outgoing* rate constants from state i. Then it is easy to see that $p_i \tau_{tr} = f_i \tau_{tr}^{(i)}$. In any given example, the α_{ij} determine the p_i and the $\tau_{tr}^{(i)}$. Then using $f_i \sim p_i / \tau_{tr}^{(i)}$ and normalization of the f_i, the f_i and τ_{tr} are easily found.

"Experimental" verification of stochastic treatment

Eqs. 2 for the *net* fluxes are well-established (2), but Eqs. 3, for the separate one-way fluxes, need verification. We have done this in special cases by an independent "mean first passage time" type of argument in which the relative probability of completing a given cycle in either direction is calculated. But here we report explicitly on numerical checks.

For this purpose we have used the four examples shown in Fig. 2, the first three of which are special cases of Fig. 1 while the fourth (Fig. 2d) is the example considered in the previous paper (3).

We have studied Fig. 2a most extensively. This model has six cycles (Fig. 1b). For this case we made 10 different computer runs of 10^5 transitions each, starting each run (arbitrarily) in state 3 (Fig. 1a). Each transition from one state to another was determined by a random number generator, with relative probabilities for the final state assigned in accordance with the various outgoing rate constants from the initial state.

Suppose the initial sequence of states (Figs. 1a and 2a) in a run is 326545612. This we call the "actual record". It contains two kinds of repeats: "immediate" and "non-immediate" (in the latter case—see below—a cycle is completed). Both kinds of repeats are cancelled from the actual record, as they occur, to provide a running "effective record". Thus 326545 ("immediate" repeat of 5) becomes 3265 (effective), after cancellation of 45, and then 32656 (immediate repeat of 6) becomes 326 (effective). Finally, 32612 (*non*-immediate repeat of 2) becomes 32 (effective), after cancellation of 612. Here, with the non-immediate repeat, the cycle 2612 (i.e., a+ in Fig. 1b) has been completed. The cycle type (a+) is determined and tallied by the computer.

If the above actual record happened to continue with 653, we would reach another *non*-immediate repeat at 32653, which would become 3 (effective) after cancellation of 2653. The second cycle completed is of type b− (Fig. 1b).

The effective record on completion of each cycle is called a "remainder" (32 after a+ and 3 after b−, above). Note (see above) that the remainder is *not* dropped as further states in the actual record are considered in the process of determining the next cycle completion. It is easy to see that the above

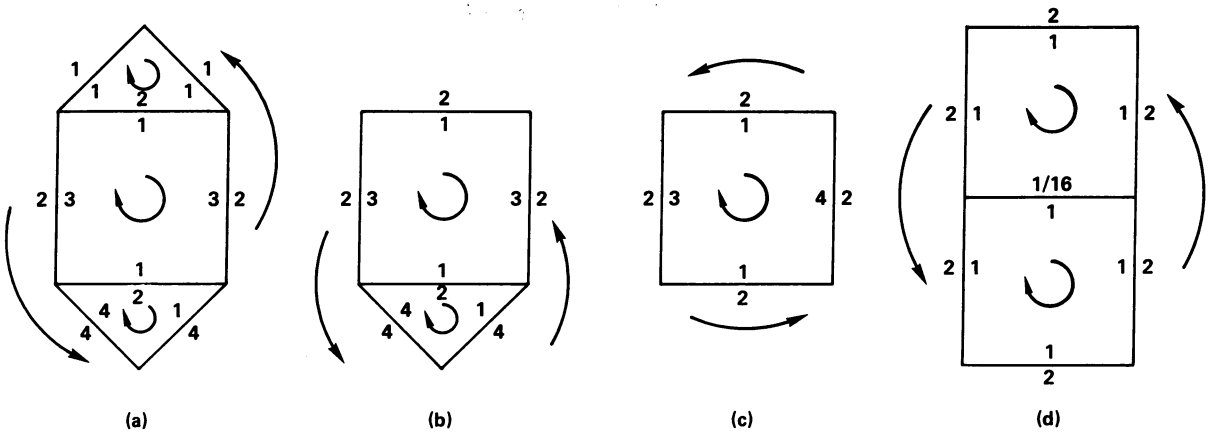

FIG. 2. Four explicit models with specified rate constants. The arrows here show the transition directions to be assigned to the various rate constants.

formal procedure records properly the actual molecular accomplishments (transport, reaction, etc.) of the system being followed (via the "actual record" of states).

We return now to the 10 computer runs based on Figs. 1 and 2a. The theoretical state probabilities (designated p_i^{th}) are most easily calculated using the method described previously (3), that is, from flux diagrams rather than from directional diagrams. These values are given in Table 1, along with $\tau_{tr}^{(i)}$. These two columns then give f_i^{th} and also $\tau_{tr} = 0.205028$ for the mean time between transitions. The last column in Table 1 contains the "experimental" p_i (for the 10 runs combined) based on the observed f_i (relative frequency of state i in the actual records) and $\tau_{tr}^{(i)}$. There is close agreement between p_i and p_i^{th}, as expected. Note that the experimental time is introduced via the *mean* times $\tau_{tr}^{(i)}$ (5) only.

The second and third columns in Table 2 show the calculation of the twelve cycle rate constants $k_{n\pm}$ from Eqs. 3, based on Figs. 1 and 2a, where $n\pm$ is the cycle index. The value of Σ is found in the p_i^{th} calculation (above) to be 4641. From Eq. 5b, $\tau = 4641/2152 = 2.15660$. The theoretical number of transitions per cycle completed is then $\tau/\tau_{tr} = 10.5186$ (experimental, Table 2 = $10^6/95249 = 10.499$). The last three columns in Table 2 refer to the ten runs *combined* (10^6 transitions). The expected (theoretical) number of cycles of each type is $\bar{r}_{n\pm}^{th}$ (fourth column). The *total* expected number of cycles is $10^6\tau_{tr}/\tau = 95070.1$. The fraction of these cycles of type a+ is then expected to be $p_{a+}^{th} = 148/2152$ (second column), etc. That is, $\bar{r}_{a+}^{th} = 10^6\tau_{tr}p_{a+}^{th}/\tau$, etc. The *observed* number of cycles of each type is $r_{n\pm}$ (fifth column). One can see at a glance that the agreement with the $\bar{r}_{n\pm}^{th}$ values confirms Eqs. 3.

To be more quantitative about this agreement: the last column in Table 2 gives $\Delta_{n\pm} = (r_{n\pm} - \bar{r}_{n\pm}^{th})/\sigma_{n\pm}^{th}$, that is, the observed deviation from the expected mean relative to the standard deviation of the expected Gaussian distribution (Eq. 6). The mean of the 12 values of $|\Delta_{n\pm}|$ is 0.617. The theoretical mean, for a very large number of values with a Gaussian distribution, is $(2/\pi)^{1/2} = 0.798$.

The above paragraph can be reinforced by calculating $\Delta_{n\pm}$ for the 10 *separate* runs of 10^5 transitions each. We find in this case that the mean of the 120 values of $|\Delta_{n\pm}|$ is 0.806. Furthermore, a tabulation of the 120 separate $\Delta_{n\pm}$ values in intervals of 0.50 about zero produces quite respectable overall agreement with the expected Gaussian distribution.

As a further check, differences between experimental cycle numbers of each type in successive runs (1–2, ···, 9–10) were used rather than deviations from expected means, as above. That is, the 60 quantities $\delta_{a+}^{12} = (r_{a+}^{(1)} - r_{a+}^{(2)})/\sigma_{a+}^{th}$, $\delta_{a+}^{34} = (r_{a+}^{(3)} - r_{a+}^{(4)})/\sigma_{a+}^{th}$, etc., were calculated. The mean of their absolute values was found to be 1.095. The theoretical mean is $2/\pi^{1/2} = 1.128$.

We have analyzed in similar fashion various linear combinations of cycle numbers, such as $r_{a+} - r_{a-}$, $r_{a+} + r_{ab+} + r_{abc+}$, etc., also with the expected results (see Eqs. 7). We omit details since these are not independent data.

Other Examples. Similar results confirming the stochastic treatment above were found for other models. For the model in Fig. 2b (three cycles), one run of 10,000 cycle completions was made. The theoretical number of transitions per cycle

TABLE 1. *Properties of states (Fig. 2a)*

State	p_i^{th}	$\tau_{tr}^{(i)}$	f_i^{th}	p_i
1	0.17841	1/2	0.07316	0.17858
2	0.20599	1/4	0.16893	0.20637
3	0.11463	1/9	0.21152	0.11473
4	0.08985	1/8	0.14737	0.08978
5	0.26029	1/4	0.21347	0.25984
6	0.15083	1/6	0.18555	0.15070

TABLE 2. *Properties of cycles (Fig. 2a)*

Cycle, $n_\pm$	$\Pi_{n\pm}\Sigma_n$	$k_{n\pm}$	$\bar{r}_{n\pm}^{th}$	$r_{n\pm}$	$\Delta_{n\pm}$
$a+$	148	0.031890	6538.3	6656	+1.456
$a-$	296	0.063779	13076.5	13019	−0.503
$b+$	256	0.055161	11309.5	11210	−0.936
$b-$	144	0.031028	6361.6	6409	+0.594
$c+$	496	0.106874	21912.1	22027	+0.776
$c-$	248	0.053437	10956.1	10880	−0.727
$ab+$	64	0.013790	2827.3	2833	+0.107
$ab-$	72	0.015514	3180.8	3195	+0.252
$bc+$	256	0.055161	11309.5	11364	+0.512
$bc-$	72	0.015514	3180.8	3235	+0.961
$abc+$	64	0.013790	2827.3	2816	−0.213
$abc-$	36	0.007757	1590.4	1605	+0.366
Total	2152	0.463695	95070.2	95249	

TABLE 3. *Effect of added states (Fig. 2b)*

Cycle	$\bar{r}_{n\pm}{}^{th}$	$r_{n\pm}$ (2)	$r_{n\pm}$ (432)	$\overline{\lvert\delta\rvert}$
$b+$	1885.4	1875	1922	0.82
$b-$	1060.5	1075	1096	
$c+$	3063.8	2972	3045	
$c-$	1531.9	1511	1558	
$bc+$	1885.4	1871	1850	
$bc-$	530.3	524	529	
Total	9957.3	9828	10,000	

completed is 11.675; observed = 11.627. The mean of the six values of $|\Delta_{n\pm}|$ was found to be 0.64.

For the model in Fig. 2c (a single cycle), eight runs of 10^5 transitions each were made: transitions per cycle (theoretical) = 17.571 (!), observed (eight runs combined) = 17.594; mean of 16 values of $|\Delta_{n\pm}| = 0.704$.

For the model in Fig. 2d (three cycles), one run of 20,044 cycle completions was made: transitions per cycle (theoretical) = 12.700, observed = 12.669; mean of six values of $|\Delta_{n+}| = 1.07$.

Conclusion. These calculations confirm that the simple separation of each mean net flux around a cycle into two mean one-way fluxes, as in Eqs. **3**, is correct. Furthermore, for a system observed over a long time interval, each possible kind of cycle completion ($\alpha+$, $\alpha-$, $\beta+$, etc.) can be treated as an independent random event with its own rate constant $k_{\alpha+}$, $k_{\alpha-}$, etc. (each k being a known function of the elementary rate constants α_{ij}).

Sensitivity of computational fluctuations in cycle numbers to added states

In this section we report on an interesting computational property of diagrams that, however, has limited significance for the simulation of experimental behavior. An example: suppose we use (in Fig. 2a) an "actual record" of, say, 10^5 states (selected by the random number generator), starting with state 3, and then alter this record merely by adding the two states 12 to the beginning of the sequence (so that there are 100,002 states in the altered sequence). We could, instead, have added one state, or three, etc. The result of this seemingly trivial change is that the cycle numbers $r_{n\pm}$ obtained (by the procedure described above) from the original actual record represent a significantly different set of fluctuations about the $\bar{r}_{n\pm}{}^{th}$ than the $r_{n\pm}$ obtained from the altered actual record. One might have expected that corresponding pairs of $r_{n\pm}$ values from the two records would differ by zero or perhaps ±1, ±2, etc., but the differences are *much* larger than this (see Table 3 below). The effect of the two added states on cycle completions and types propagates itself, so to speak, through the entire actual record, producing a quite different pattern of cycle completions. The reader can easily verify this by concocting a more or less realistic sample sequence of, say, 50 states with 5–10 cycle completions.

However, this computational cycle bookkeeping phenomenon is no more than trivially significant for fluctuations in cycle numbers of experimental systems. This follows from the fact that experiments are carried out on a large ensemble of systems (rather than on a single system), with consequent averaging over, among other things, all possible starting states and a different sequence of states ("actual record") for each system in the ensemble.

TABLE 4. *Cycle combinations from Table 3*

	r (2)	r (432)	$\overline{\lvert\delta\rvert}$
$(b+) - (b-)$	800	826	0.46
$(c+) - (c-)$	1461	1487	
$(bc+) - (bc-)$	1347	1321	
$B+ \equiv (b+) + (bc+)$	3746	3772	0.74
$B- \equiv (b-) + (bc-)$	1599	1625	
$C+ \equiv (c+) + (bc+)$	4843	4895	
$C- \equiv (c-) + (bc-)$	2035	2087	
$(B+) - (B-)$	2147	2147	0.00
$(C+) - (C-)$	2808	2808	

Tables 3 and 4 present a particular example (also used in the preceding section), based on Fig. 2b (three cycles, labeled as in Fig. 1b). First, a run of 10,000 cycles, requiring a sequence of 116,266 states, was made from a starting sequence 432 (states labeled as in Fig. 1a). Then the same random numbers (and hence the same sequence of states) were used starting with state 2 (i.e., omitting 43), for a total sequence of 116,278 states (i.e., 116,264 plus completion of the last cycle). The two observed sets of cycle numbers $r_{n\pm}$ are quite different (Table 3). The number $\overline{|\delta|} = 0.82$ in Table 3 is the mean of the six absolute values of $\delta_{b+} \equiv (r_{b+}{}^{(2)} - r_{b+}{}^{(432)})/\sigma_{b+}{}^{th}$, etc. For a large number of *uncorrelated* differences of this type we would expect (see above) $\overline{|\delta|} = 2/\pi^{1/2} = 1.128$. We see here, and this is confirmed in the more extensive example below, that there is some degree of correlation between $r_{n\pm}{}^{(2)}$ and $r_{n\pm}{}^{(432)}$, but much less than the virtually complete correlation ($\overline{|\delta|} \cong 0$) that might have been expected.

Since complete correlation between the two sets of $r_{n\pm}$ is not found, one might then expect it between the two sets of *net* cycle numbers $r_{n+} - r_{n-}$. The top three rows of Table 4 show that this is not the case, though the degree of correlation increases ($\overline{|\delta|} = 0.46$ is an average of three values; $\sigma_n{}^{th}$ used here follows from Eq. **7b**).

Individual cycle fluxes (one-way or net) are not observable quantities in multicycle models such as Fig. 2b. Observable fluxes would obviously be associated here with the cycle combinations $B \equiv b + bc$ and $C \equiv c + bc$. Thus, in the next four rows of Table 4, we try the one-way cycle numbers $B+$, etc. (ensemble averages of these "operational" fluxes, in membrane transport systems, could be measured with the aid of radioactive tracers). Again there is only partial correlation ($\overline{|\delta|} = 0.74$) between the two sets 2 and 432. But, finally (Table 4) when we use the cycle numbers associated with the *net* "operational" combinations $(B+) - (B-)$ and $(C+) - (C-)$, we find complete correlation (i.e., the sets 2 and 432 give the same cycle numbers, though they might have differed by ±1).

Equivalent results were also found for the three models in Figs. 2a, c, and d. In the Fig. 2a case, the ten runs (Table 2) of 10^5 states each, all with starting state 3, were repeated using the same ten sequences of states but with starting states 123. The mean of the 120 absolute values of $\delta_{a+} = (r_{a+}{}^{(3)} - r_{a+}{}^{(123)})/\sigma_{a+}{}^{th}$ (10 runs), etc., was found to be $\overline{|\delta|} = 0.748$ (compare the uncorrelated value, 1.128). For the differences in the two sets (3; 123) of *net* cycle numbers $r_{n+} - r_{n-}$, the

TABLE 5. *Numbers of cycles following remainders (Fig. 2a)*

Rem.	$a+$	$a-$	$bc+$	$bc-$	$abc+$	$abc-$
1	494	967	717	206	192	103
12	467	198	364	120	182	17
16	81	845	381	94	41	87
123	191	80	415	47	176	13
165	48	449	214	117	12	111
1265	128	8	29	69	12	1
1623	1	191	233	5	1	2
Total	1410	2738	2353	658	616	334
$\bar{r}_{n\pm}{}^{th}$	1375	2751	2379	669	595	335

TABLE 6. *Numbers of remainders following cycles (Fig. 2a)*

Rem.	$b+$	$b-$	$bc+$	$bc-$	$c+$	$c-$	Total
12	1142	670	1154	331	—	—	3297
16	1198	736	1199	327	—	—	3460
123	—	—	—	—	1742	865	2607
165	—	—	—	—	1864	860	2724
1265	—	—	—	—	416	243	659
1623	—	—	—	—	577	293	870
Total	2340	1406	2353	658	4599	2261	
$\bar{r}_{n\pm}{}^{th}$	2379	1338	2379	669	4610	2305	

mean of 60 absolute values was $\overline{|\delta|} = 0.626$. For the 60 *one-way* "operational" combinations $A \equiv a + ab + abc$, $B \equiv b + ab + bc + abc$, $C \equiv c + bc + abc$, $\overline{|\delta|} = 0.508$. Note that the correlation becomes stronger in successive cases. Finally, as above, for the *net* operational combinations $(A+) - (A-)$, etc., $\overline{|\delta|} \cong 0.00$ (all 30 differences in cycle numbers are 0 or ± 1).

Stochastic analysis of cycles for shorter time intervals

We have seen that the cycle rate constants $k_{n\pm}$ suffice for a stochastic analysis of cycle completions over a long time interval (large numbers of cycles). But the kinetics of individual cycle completions requires more detail. This would be necessary, for example, in the treatment of noise associated with cycle fluxes (say in active transport) over the complete frequency range. No analytical theory is available at this level. We merely present a numerical (Monte Carlo) example here in the hope of stimulating future work on a proper analytical theory.

We have seen that there is a "remainder" (the effective record)—a short sequence of states—after each cycle completion. There are four essential points to be made: (*a*) after a cycle completion of type c' with remainder r', the probability that the next completed cycle c'' will be of any given cycle type depends on r' (but all cycle types are *possible* after any kind of remainder); (*b*) the mean time required for completion of c'' (counting from c') also depends on r'; (*c*) the probability that a given type of remainder will occur depends on the kind of cycle being completed and also on the immediately preceding remainder (in fact, each cycle type permits of only certain remainders); and (*d*) an average over all possible starting states (i.e., over all states in the diagram) is essential because each starting state is necessarily the starting state in all remainders that occur in a given sequence of states (actual record) and thus each starting state has its own and exclusive set of possible remainders.

To recapitulate partially: in the sequence r(remainder)-c(cycle) $rcrc \ldots$, each c has a "memory" of the preceding r and each r has a "memory" of the preceding rc. In contrast, the simple (long time) theory at the beginning of this paper includes no memory effect at all.

We turn now to an example that illustrates some but not all of the points above. We use the model in Fig. 2a again and arbitrarily select state 1 as the starting state. The reader can easily verify that the only possible remainders are then 1, 12, 16, 123, 165, 1265, and 1623. Also, it is easy to see that (with starting state 1): cycle types $a\pm$, $ab\pm$, and $abc\pm$ can leave only the remainder 1; $b\pm$ and $bc\pm$ can leave only 12 and 16; and $c\pm$ can leave only 123, 165, 1265, and 1623.

We made a single run of 20,000 cycles that started with state 1 and happened to end with the remainder 1265. The computer recorded (*i*) the numbers of completed cycles of each type that followed each kind of remainder, and (*ii*) the number of remainders of each type that followed each kind of cycle. For simplicity in this example, the time was not considered nor did we subdivide the cycle types in (*ii*) according to the preceding remainder (as must be done in a complete analysis).

Table 5 gives illustrative, partial results (six of the twelve cycle types) on (*i*) while Table 6 presents the data on (*ii*) (omitting $a\pm$, $ab\pm$, and $abc\pm$; see above). It is evident from Table 5 that the relative probability of different cycle types is indeed different for different remainders. If we had subdivided cycle types according to the preceding remainder, Table 6 would require a third dimension.

A proper theory would provide (for a given diagram and for each starting state), as functions of the α_{ij}, the *probability* of each type of remainder following each kind of cycle and preceding remainder and the *rate constant* $k_{n\pm}{}^{(rem)}$ for each type of cycle following each kind of remainder. With these available, the elementary transitions $i \to j$ could be by-passed in following the stochastics of individual cycle completions. The $k_{n\pm}$ used earlier in the paper are, in the most general case, averages of $k_{n\pm}{}^{(rem)}$ over different starting states and over different remainders for each starting state.

1. Hill, T. L. (1974) *Progr. Biophys. Mol. Biol.* **28**, 267–340.
2. Hill, T. L. (1968) *Thermodynamics for Chemists and Biologists* (Addison-Wesley, Reading, Mass.).
3. Hill, T. L. (1975) *Biochemistry*, in press.
4. King, E. L. & Altman, C. (1956) *J. Phys. Chem.* **60**, 1375–1378.
5. Gordon, R. (1968) *J. Chem. Phys.* **49**, 570–580.